# Mutation of the Mouse Hepatocyte Nuclear Factor/Forkhead Homologue 4 Gene Results in an Absence of Cilia and Random Left-Right Asymmetry

**Jianchun Chen, Heather J. Knowles, Jennifer L. Hebert, and Brian P. Hackett**

*The Edward Mallinckrodt Department of Pediatrics, Washington University School of Medicine, St. Louis, Missouri 63110*

## Abstract

**Winged helix transcription factors play important roles in cellular differentiation and cell-specific gene expression. To define the role of the winged helix factor hepatocyte nuclear factor/forkhead homologue (HFH)-4, a targeted mutation was created in the mouse *hfh-4* gene. No expression of HFH-4 was detected in *hfh-4*$^{-/-}$ mice by RNA blot analysis, in situ hybridization, or RT-PCR. *hfh-4*$^{-/-}$ mice were noted to have abnormalities of organ *situs* consistent with random determination of left-right asymmetry. In addition, a complete absence of cilia was noted in *hfh-4*$^{-/-}$ mice. The *hfh-4* gene is thus essential for nonrandom determination of left-right asymmetry and development of ciliated cells. Homozygous mutant mice also exhibited prenatal and postnatal growth failure, perinatal lethality and, in some cases, hydrocephalus. RT-PCR revealed an absence of *left-right dynein* (*lrd*) expression in the embryonic lungs of *hfh-4*$^{-/-}$ mice, suggesting that HFH-4 may act by regulating expression of members of the dynein family of genes. The abnormalities in ciliary development and organ *situs* in *hfh-4*$^{-/-}$ mice are similar to those observed in human congenital syndromes such as Kartagener syndrome. Targeted mutation of *hfh-4* thus provides a model for elucidating the mechanisms regulating ciliary development and determination of left-right asymmetry. (*J. Clin. Invest.* 1998. 102:1077–1082.) Key words: winged helix • *situs* • cilia • left-right asymmetry • dynein**

## Introduction

Organ position along the left-right body axis is genetically determined during vertebrate development in a conserved, nonrandom fashion. Human defects in organ position, or *situs*, are estimated to occur in 1:10,000 live births (1). Defects in cardiac morphogenesis associated with these defects in laterality may result in lethal congenital heart malformations (1). In certain

Address correspondence to Brian P. Hackett, Department of Pediatrics, Washington University School of Medicine, One Children's Place, St. Louis, MO 63110. Phone: 314-454-6148; FAX: 314-454-4633; E-mail: hackett@kids.wustl.edu

congenital syndromes, such as Kartagener syndrome, abnormalities of organ *situs* may be associated with defects in the development of cilia. Kartagener syndrome classically has been characterized by the triad of bronchiectasis, chronic sinusitis, and *situs inversus*. The chronic respiratory disease and, in some cases, infertility can be attributed to ciliary dysfunction. The mechanisms resulting in *situs inversus* are less clear. Kartagener syndrome belongs to a group of syndromes characterized by primary ciliary dyskinesia. Determination of left-right asymmetry in these syndromes appears to be random; consequently only half of affected individuals will have *situs inversus* (2). Although inheritance is generally thought to be autosomal recessive, genetic evidence suggests that mutations in multiple genes may result in a similar final phenotype of Kartagener syndrome (2).

Human genetic syndromes, such as Kartagener syndrome, and animal models, such as the WIC-Hyd rat, have demonstrated a relationship between the determination of left-right asymmetry and the development of ciliated cells (3, 4). However, the specific genes involved remain unidentified The asymmetric expression of genes, such as *nodal*, *lefty-1*, and *lefty-2*, in the developing mammalian embryo suggests potential molecular mechanisms regulating the determination of left-right asymmetry (5–8). In the *inversus viscerum* (*iv*)[1] mouse, which exhibits random determination of left-right asymmetry, the normally asymmetric patterns of expression of these genes are disrupted (5–9). The gene mutated in the *iv* mouse has been identified recently as a member of the dynein family of genes and has been termed *left-right dynein* (*lrd*) (10). Members of the dynein family are thus essential for both the development of cilia and the determination of left-right asymmetry (10, 11). However, examination of *iv* mice has revealed apparently normal cilia (12).

The winged helix family of transcription factors is characterized by a 110–amino acid DNA binding domain termed the winged helix domain based on its three dimensional x-ray crystallographic structure (13). Alternatively, this family of proteins has been referred to as the forkhead family based on the appearance of *Drosophila* embryos with mutations in a *Drosophila* family member (14). More than 80 family members have been identified in metazoan organisms and several of these have been shown to play important roles in cell fate determination and cell-specific gene expression (15). Hepatocyte

nuclear factor/forkhead homologue (HFH)-4 is a 421–amino acid member of the winged helix family (16, 17). Expression of HFH-4 in mice and humans has been localized to the lung, spermatids, oviduct, choroid plexus, and fetal kidney (17–19). In the developing mouse and human lung, HFH-4 expression is restricted to the proximal pulmonary epithelium and is associated with the differentiation of the proximal from the distal respiratory epithelium during the late pseudoglandular stage of lung development (17, 19). Expression of HFH-4 is also developmentally regulated in spermatids, choroid plexus, and renal epithelium (17–19). These tissues are all sites of ciliated cells consistent with a role for HFH-4 in the differentiation of ciliated epithelium. We report here that targeted disruption of the mouse *hfh-4* gene demonstrates an essential role for HFH-4 in the development of cilia and, in addition, the nonrandom determination of left-right asymmetry.

## Methods

*Targeted disruption of the mouse hfh-4 gene.* A 10-kb clone of the mouse *hfh-4* gene was obtained by screening a 129SvJ mouse genomic library with a [32P]cDNA probe to the 5′ region of the mouse HFH-4 cDNA (Fig. 1 *a*) as described previously (20). A targeting vec-

tor was constructed by replacement of an XhoI–XbaI fragment of the mouse *hfh-4* gene, which includes the first exon, with the phosphoglycerate kinase/neomycin resistance gene (Fig. 1 *a*). The replacement cassette was then subcloned into the HindIII site of a pBluescript plasmid containing the HSV-thymidine kinase gene (Fig. 1 *a*).

25 μg of linearized targeting vector DNA was electroporated into 10⁷ R1 embryonic stem (ES) cells (21). Cell lines were established by selection of ES clones by growth in the presence of G418 and ganciclovir and then analyzed by Southern blot for homologous recombination at the *hfh-4* locus. Correctly targeted clones were injected into C57BL/6J blastocysts and the blastocysts were transferred to pseudopregnant (C57BL/6 × CBA) F₁ hybrid females. Chimeric mice were identified by the presence of agouti pigmentation in the coat and confirmed by Southern blot analysis of genomic DNA isolated from tail segments. Chimeric males were mated with Black Swiss female mice and offspring carrying the targeted allele were identified by Southern blot analysis. Heterozygous animals were mated and the genotype of offspring was determined by PCR.

*Southern blot analysis.* Genomic DNA was isolated from proteinase K digests of ES cells or tail segments. DNA was digested with Tth111I, electrophoresed, and transferred to a nylon membrane. The membrane was hybridized with a [32P]cRNA probe to the region of *hfh-4* indicated by *a* in Fig. 1 *a*. The wild-type allele yields a 6.0-kb restriction fragment and the mutated allele yields a 4.2-kb restriction fragment (Fig. 1 *a*).
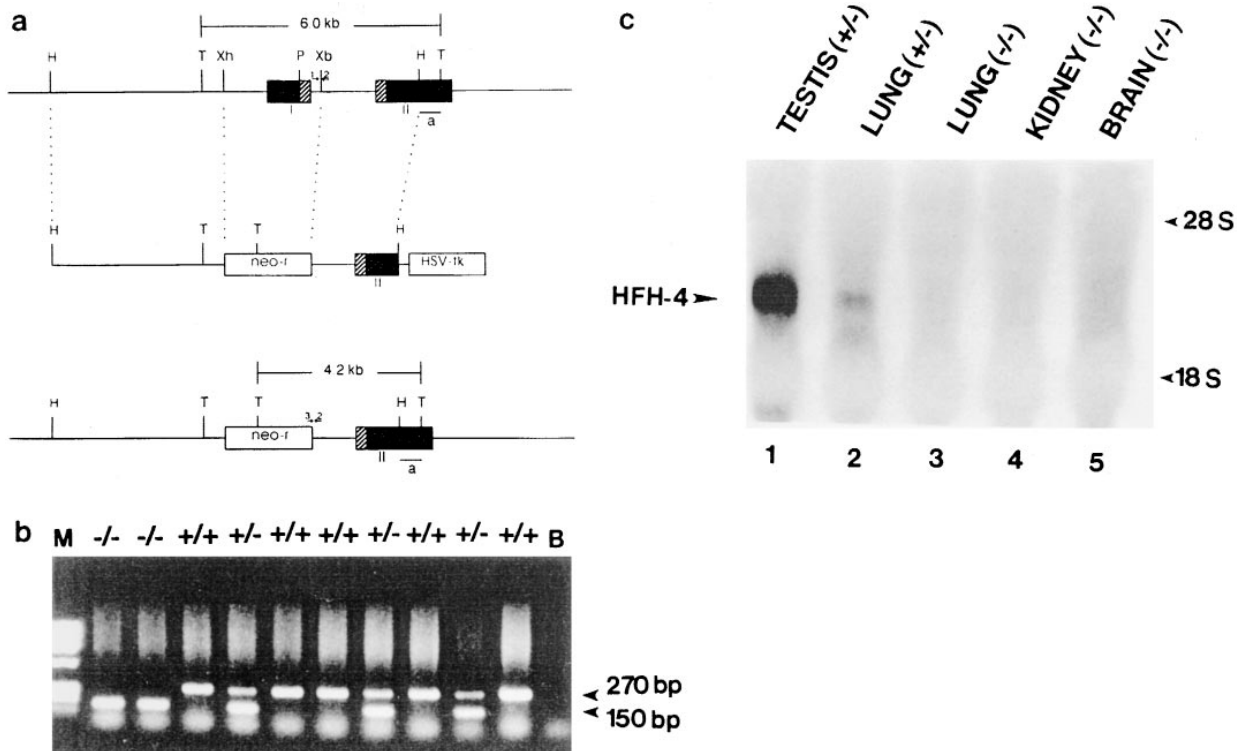


*Figure 1.* Targeted disruption of the mouse *hfh-4* gene. (*a*) Wild-type *hfh-4* allele (*top*) is composed of two exons (*solid boxes*) with the DNA-binding domain (*shaded boxes*) split between exons I and II. In the targeting vector (*middle*), the first exon has been replaced with the pgk-neomycin resistance gene (*neo-r*). The HSV thymidine kinase gene (*HSV-tk*) is included outside the region of homology. In the mutant allele (*bottom*), replacement of exon I results in disruption of the DNA-binding domain. (*b*) PCR analysis of genomic DNA isolated from offspring of a heterozygous mating. Tail segments were digested overnight with proteinase K and genomic DNA was isolated. PCR was performed with genomic DNA using oligonucleotide primers 1, 2, and 3 as in *a*. The wild-type allele is expected to generate a 270-bp amplification product and the targeted allele a 150-bp fragment. (*c*) RNA blot analysis of HFH-4 expression. 20 μg of total RNA was isolated from the indicated organs and hybridized with a [32P]cRNA probe to the 3′ region of the mouse HFH-4 cDNA. *H*, HindIII; *T*, Tth111I; *Xh*, XhoI; *Xb*, XbaI; *P*, PmaI; 6.0- and 4.2-kb bars indicate Tth111I restriction fragments used to identify the wild-type and mutant allele by Southern blot analysis; *a*, location of probe for Southern blot analysis. Arrows 1, 2, and 3 indicate the locations of oligonucleotide primers for PCR identification of wild-type and mutant *hfh-4* alleles. +/+, wild-type; +/−, heterozygous mutant; −/−, homozygous mutant.

*PCR.* For PCR identification of wild-type and mutant *hfh-4* alleles, genomic DNA was isolated from tail digests as above. Oligonucleotide primers used for amplification as shown in Fig. 1 *a* are: 1 = 5′-CCAATGGGCCAGGCTGCCGTG-3′; 2 = 5′-CGTGCCCTCT-TGCTCCTTGG-3′; and 3 = 5′-CTGCTAAAGCGCATGCTC-3′. 28 cycles of amplification were performed with denaturing at 94°C for 1 min, annealing at 60°C for 2 min, and elongation at 72°C for 3 min. The wild-type allele was identified by the presence of a 270-bp product and the mutant allele by the presence of a 150-bp product.

*RNA isolation and RNA blot analysis.* Organs were flash-frozen in liquid nitrogen and total RNA was isolated with an Rneasy spin column (Qiagen, Valencia, CA). RNA samples were denatured, electrophoresed, and transferred to nylon (Hybond-N; Amersham, Arlington Heights, IL) as described previously (22). Blots were hybridized at 58.5°C with a [$^{32}$P]cRNA probe to the 3′ region of the mouse HFH-4 cDNA followed by washing and exposure to film as before (22). Antisense [$^{32}$P]cRNA probes were synthesized from linearized plasmid templates as described (22).

*Organ isolation, preparation, and histology.* Organs were isolated en bloc and fixed in 10% (vol/vol) buffered formalin as described previously (17). After dehydration in ethanol, tissues were embedded in paraffin, cut onto slides, and stained with hematoxylin and eosin.

*RT-PCR.* SuperScript reverse transcriptase (GIBCO BRL, Gaithersburg, MD) was used for cDNA preparation from total RNA isolated from the lungs of embryonic day (e) 18.5 mice. PCR amplification was performed using gene specific primers: 5′-ACAGGAGAGG-GAAGGCTGGGG-3′ and 5′-GCGGCCATGGACTGTGAGATC-CAC-3′ for HFH-4; 5′-AGAGCTTCATCCTCAAAGTTGTCC-3′ and 5′-CAACTGGCCACATACGGATTC-3′ for *lrd* (10); and 5′-ATGGATGACGATATCGCT-3′ and 5′-TGTTGAAGGTCTCA-AACA-3′ for β-actin. 25 cycles of amplification were performed with denaturing at 94°C for 30 s, annealing at 62°C for 30 s and elongation at 72°C for 2 min.

## Results

*Targeted disruption of the mouse hfh-4 gene.* Correctly targeted ES cells were identified by Southern blot analysis (data not shown). Despite postmeiotic expression of HFH-4 in haploid spermatids, chimeric and *hfh-4$^{+/-}$* males were fertile and homozygous mutant mice were obtained from matings of *hfh-4$^{+/-}$* males and females (Fig. 1 *b*). By RNA blot analysis, RT-PCR, and in situ hybridization, no HFH-4 expression was detected in tissues from *hfh-4$^{-/-}$* mice (Fig. 1 *c* and data not shown, also see Fig. 4 *c*).

*Growth failure and perinatal lethality in hfh-4$^{-/-}$ mice.* Litters from matings of heterozygous mice included *hfh-4$^{-/-}$* offspring readily distinguished from their littermates by their smaller size and poor postnatal weight gain (Fig. 2). There was no significant difference in the mean weights of *hfh-4$^{+/+}$* and *hfh-4$^{+/-}$* mice at any age (data not shown). To determine the timing of the onset of growth failure, embryonic weights were obtained beginning at e12.5. By e16.5, a significant difference was noted in the mean embryonic weight of *hfh-4$^{-/-}$* mice versus *hfh-4$^{+/+}$* and *hfh-4$^{+/-}$* littermates (0.610 vs. 0.708 g; $P < 0.001$ by Student's *t* test, two-tailed). Placental weights did not differ at any time during gestation (data not shown).

76 mice were genotyped at 2–3 wk of age and only two (2.6%) *hfh-4$^{-/-}$* mice were identified. Before 2 wk of age, dead or dying *hfh-4$^{-/-}$* mice were identified in litters with most postnatal deaths occurring during the first 4 d of life. Before death, *hfh-4$^{-/-}$* mice were less active than their littermates and had a wasted appearance; no respiratory distress was noted. To determine if the *hfh-4$^{-/-}$* phenotype was an embryonic lethal,
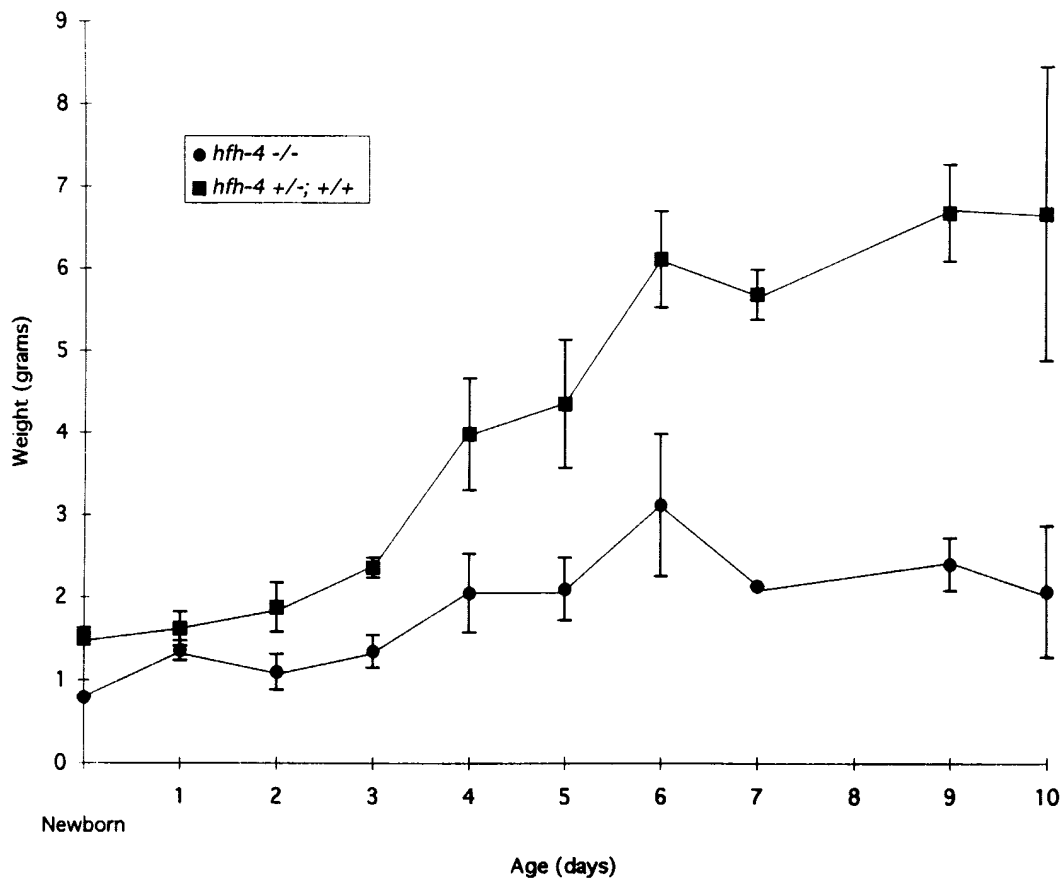


*Figure 2.* Growth failure in *hfh-4$^{-/-}$* mice. Mean weights (±SD) for *hfh-4$^{-/-}$* (*circles*) and *hfh-4$^{+/-}$* plus *hfh-4$^{+/+}$* (*squares*) mice.

## Table I. Genotypes of Embryos from Heterozygous Matings

| Gestation | Genotype | | |
|---|---|---|---|
| | +/+ | +/− | −/− |
| e12.5 | 9 (18.4%) | 25 (51.0%) | 15 (30.6%) |
| e14.5 | 14 (34.1%) | 17 (41.4%) | 10 (24.4%) |
| e16.5 | 7 (35.0%) | 10 (50.0%) | 3 (15.0%) |
| e18.5* | 27 (31.4%) | 48 (55.8%) | 11 (12.8%) |

*$\chi^2 = 7.50$; $P < 0.025$.

genotypes of embryos were determined by PCR amplification of genomic DNA (Table I). By $\chi^2$ analysis, a significant loss of $hfh\text{-}4^{-/-}$ mice is observed between e16.5 and e18.5. Also, of six dead embryos genotyped at e18.5 before resorption, all were homozygous for the targeted allele. A single $hfh\text{-}4^{-/-}$ female and two $hfh\text{-}4^{-/-}$ males survived to beyond 12 wk of age and remained healthy appearing despite being smaller than their wild-type and heterozygous littermates. Attempts to mate these animals with demonstrated fertile wild-type animals were unsuccessful.

*Abnormalities of organ situs and hydrocephalus in hfh-4⁻/⁻ mice.* External examination of $hfh\text{-}4^{-/-}$ pups revealed that in some pups the milk-filled stomach was located on the right side of the body. No other gross abnormalities were noted on external examination. Necropsy examination of the internal viscera of $hfh\text{-}4^{-/-}$ mice revealed three phenotypes with respect to organ *situs*: (*1*) heterotaxy with either reversal of the abdominal viscera and normal heart position or dextrocardia with normal positioning of the abdominal viscera (Fig. 3, *a* and *b*); (*2*) *situs inversus* with reversal of the abdominal organs and dextrocardia (Fig. 3 *c*); and (*3*) *situs solitus* (not shown). Of 27 $hfh\text{-}4^{-/-}$ mice examined at birth, 13 (48.1%) exhibited reversal of the abdominal viscera consistent with random determination of left-right asymmetry in $hfh\text{-}4^{-/-}$ mice. Asplenia or polysplenia was not observed. No abnormalities of *situs* were observed in $hfh\text{-}4^{+/-}$ mice. In addition to abnormalities of *situs*, hydrocephalus was observed in three of six $hfh\text{-}4^{-/-}$ mice examined at > 1 wk of age (Fig. 3, *d* and *e*).

*Absence of cilia in hfh-4⁻/⁻ mice.* HFH-4 is expressed in ciliated tissues including proximal respiratory epithelium, oviduct, haploid sperm, and choroid plexus (17, 18). Examination of these tissues in $hfh\text{-}4^{-/-}$ mice revealed a complete absence of cilia (or flagella in the case of sperm) (Fig. 4, *a* and *b*, and data not shown). Within the proximal respiratory epithelium, expression of the Clara cell secretory protein gene, a marker for nonciliated epithelial cells, was unaffected in $hfh\text{-}4^{-/-}$ mice (data not shown) (23).
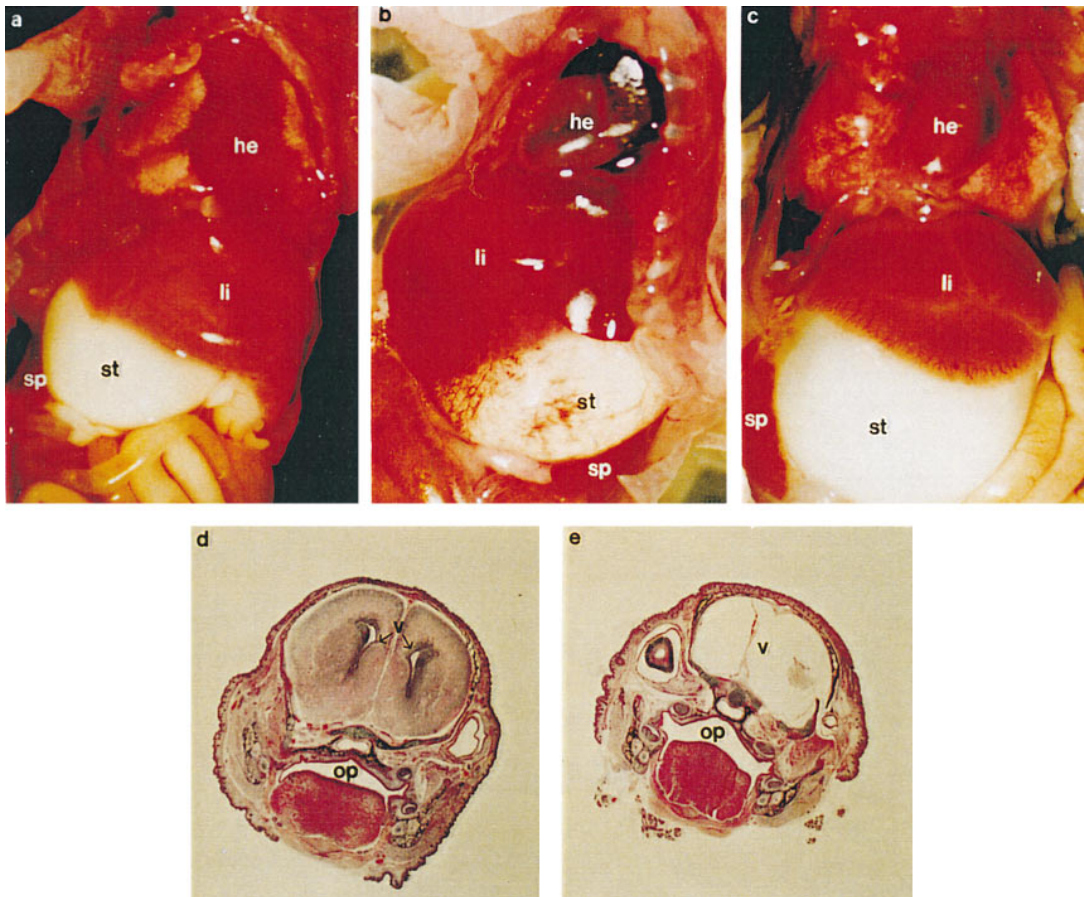


*Figure 3.* Heterotaxy and hydrocephalus in $hfh\text{-}4^{-/-}$ mice. (*a*) Reversal of abdominal viscera with normal heart position. (*b*) Dextrocardia with normal position of abdominal viscera. (*c*) Reversal of abdominal viscera with dextrocardia. (*d*) Coronal section of $hfh\text{-}4^{+/-}$ mouse brain. (*e*) Coronal section of $hfh\text{-}4^{-/-}$ mouse brain. Note enlarged ventricles (*v*) in *e*. Sections are hematoxylin and eosin stained. *sp*, spleen; *st*, stomach; *li*, liver; *he*, heart; *v*, ventricle; *op*, oropharynx.
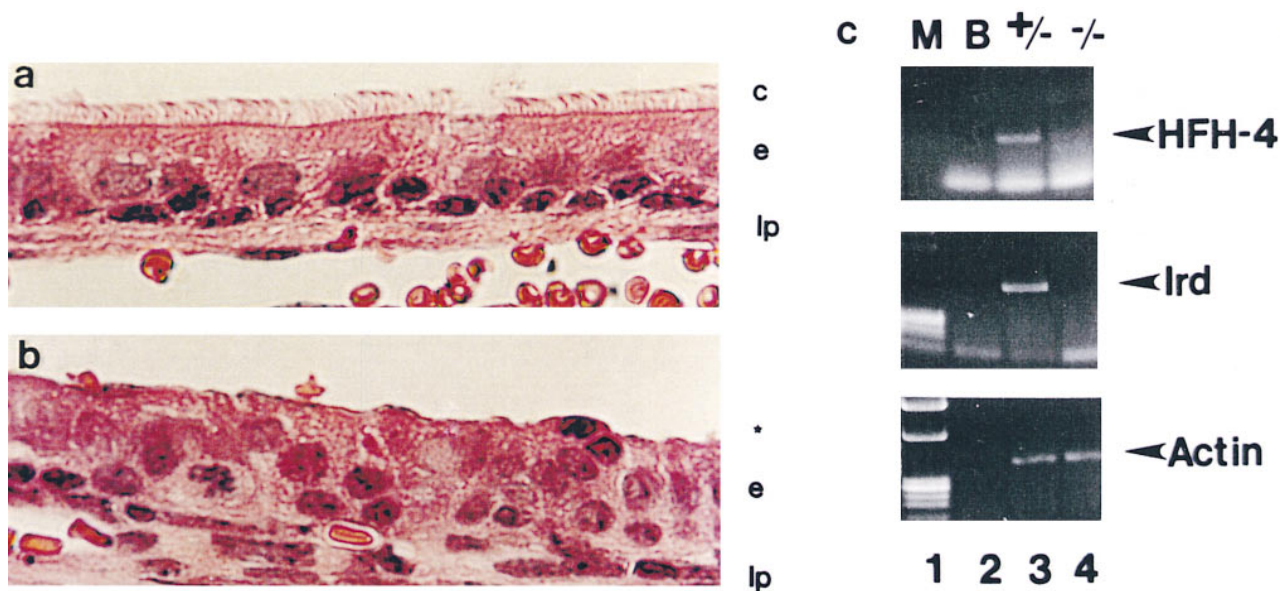
**Figure 4.** Absence of cilia in *hfh-4*$^{-/-}$ mice. Hematoxylin and eosin–stained section of nasal respiratory epithelium from *hfh-4*$^{+/-}$ mouse (*a*) and *hfh-4*$^{-/-}$ mouse (*b*). Cilia (*c*) are absent from the surface of the *hfh-4*$^{-/-}$ epithelium (*). *e*, epithelial cells; *lp*, lamina propria. (*c*) RT-PCR of total lung RNA. cDNA was prepared from e18.5 lung from *hfh-4*$^{+/-}$ (lane *3*) and *hfh-4*$^{-/-}$ (lane *4*) mice and specific primers used to amplify HFH-4, *lrd*, or β-actin. No products were obtained in the absence of RNA (*B*, lane *2*) or in the absence of reverse transcriptase (data not shown). *M*, markers (lane *1*).

Members of the dynein family of proteins are essential for both cilia formation and, as recently demonstrated for *lrd*, essential for nonrandom determination of left-right asymmetry (10, 11). Expression of the *lrd* gene was examined in *hfh-4*$^{-/-}$ mice by RT-PCR amplification of total RNA isolated from e18.5 *hfh-4*$^{+/-}$ and *hfh-4*$^{-/-}$ lung tissue (Fig. 4 *c*). Expression of *lrd* and *hfh-4* was detectable in RNA from heterozygous lung tissue (lane *3*). No expression of these genes was detected by RT-PCR amplification of RNA from the embryonic lungs of *hfh-4*$^{-/-}$ mice (lane *4*). The control β-actin expression was detected in both *hfh-4*$^{+/-}$ and *hfh-4*$^{-/-}$ lung tissue (lanes *3* and *4*). These results were confirmed with RNA isolated from the embryonic lungs of three different *hfh-4*$^{-/-}$ mice.

## Discussion

A relationship between the determination of left-right asymmetry and the development of ciliated cells has been demonstrated by human genetic syndromes, such as Kartagener syndrome, and animal models such as the WIC-Hyd rat (3, 4). The identification of a dynein gene, *lrd*, as the gene mutated in the *iv* mouse provides another link between the determination of left-right asymmetry and the dynein family of proteins (10). However, cilia structure and function have been reported to be normal in the *iv* mouse (12). The winged helix transcription factor HFH-4 is thus the first gene identified as essential for both cilia formation and the nonrandom determination of left-right asymmetry. As such, targeted disruption of the mouse *hfh-4* gene provides a unique model for human syndromes, such as Kartagener syndrome, that involve abnormalities of cilia formation and *situs*. Human syndromes involving defects in laterality have been linked to multiple chromosomal loci, suggesting the involvement of multiple genes in the determination of left-right asymmetry (24–26). The human HFH-4 gene

has been localized to chromosome 17q23-qter but as yet no pedigrees with abnormalities of *situs* and/or ciliary development have been linked to this region (19). In the majority of cases, however, genetic linkage has not been established in these syndromes (2). HFH-4 thus remains a candidate gene for mutation in human laterality syndromes with associated ciliary abnormalities.

As in the *iv* mouse, determination of left-right asymmetry is random in HFH-4–deficient mice. Asymmetry along the left-right axis is present, although the arrangement of organs along the axis may be normal or reversed. These observations are consistent with the concept of at least two genetically distinct steps in the determination of left-right asymmetry: generation of an asymmetric axis and conserved positioning of structures along the axis (27). Disruption of the asymmetric pattern of expression of genes such as *nodal*, *lefty-1*, and *lefty-2* in the *iv* mouse demonstrates that *lrd* is required for the normal asymmetric pattern of expression of these genes (5–8, 10). The absence of detectable *lrd* expression in lung tissue from *hfh-4*$^{-/-}$ mice suggests that HFH-4 may, in turn, act through regulation of expression of members of the dynein family.

Dyneins are essential for both the development of ciliated cells and the nonrandom determination of left-right asymmetry (10, 11). HFH-4 may be essential for both developmental pathways through regulation of dynein gene expression. Within cilia, dyneins act to couple hydrolysis of ATP to cilia movement (11). The mechanism by which dyneins regulate nonrandom determination of left-right asymmetry is not entirely clear. Cells with monocilia are present within the node of the developing mouse embryo (28, 29). Although it has been proposed that these cilia may function in determination of left-right asymmetry, they lack dynein arms, appear to be immotile, and have unknown functions (28, 29). In addition to the role of dyneins in cilia function, dyneins act in the cytoplasm as minus end molecular motors determining the movement of

molecules within the cytoplasm (11). The establishment of a cytoplasmic left-right gradient of molecules by cytoplasmic dyneins may translate to later organ asymmetry along the left-right body axis (30).

The lethality and growth failure observed in $hfh\text{-}4^{-/-}$ mice may in part be due to congenital defects associated with abnormalities of *situs*. A range of cardiac malformations and other organ abnormalities has been reported to be associated with defects in laterality (31–33). Similar abnormalities, in particular defects in cardiac morphogenesis, may result in the perinatal lethality observed in $hfh\text{-}4^{-/-}$ mice. The contribution of hydrocephalus to mortality is unknown, although one of three mice exhibiting hydrocephalus expired at 4 wk of age. Hydrocephalus has been reported previously in association with ciliary abnormalities in both humans and in the WIC-Hyd rat (2, 34). As in $hfh\text{-}4^{-/-}$ mice, the penetrance of hydrocephalus is not complete and suggests a role for ciliary movement in cerebrospinal fluid dynamics (34). Members of the winged helix family of transcription factors have also been implicated in the regulation of genes involved in growth and metabolism in both vertebrates and *Caenorhabidtis elegans* (35–38). Disruption of these metabolic and growth regulatory pathways in $hfh\text{-}4^{-/-}$ mice may contribute to growth failure in addition to growth failure secondary to congenital organ defects.

## Acknowledgments

## References

1. Burn, J. 1991. Disturbance of morphological laterality in humans. *Ciba Found. Symp.* 162:282–299.

2. Afzelius, B.A., and B. Mossberg. 1995. Immotile-cilia syndrome (primary ciliary dyskinesia), including Kartagener syndrome. *In* The Metabolic and Molecular Bases of Inherited Disease. Vol. 3. C.R. Scriver, A.L. Beaudet, W.S. Sly, and D. Valle, editors. McGraw-Hill, Inc., New York. 3943–3954.

3. Afzelius, B. 1995. Situs inversus and ciliary abnormalities. What is the connection? *Int. J. Dev. Biol.* 39:839–844.

4. Torikata, C., C. Kijimoto, and M. Koto. 1991. Ultrastructure of respiratory cilia of WIC-Hyd male rats. An animal model for human immotile cilia syndrome. *Am. J. Pathol.* 138:341–347.

5. Meno, C., Y. Ito, Y. Saijoh, Y. Matsuda, K. Tashiro, S. Kuhara, and H. Hamada. 1997. Two closely-related left-right asymmetrically expressed genes, *lefty-1* and *lefty-2*: their distinct expression domains, chromosomal linkage and direct neuralizing activity in *Xenopus* embryos. *Genes Cells.* 2:513–524.

6. Meno, C., Y. Saijoh, F. Hideta, M. Ikeda, T. Yokoyama, M. Yokoyama, Y. Toyoda, and H. Hamada. 1996. Left-right asymmetric expression of the TGFβ-family member *lefty* in mouse embryos. *Nature.* 381:151–158.

7. Collignon, J., I. Varlet, and E.J. Robertson. 1996. Relationship between asymmetric *nodal* expression and the direction of embryonic turning. *Nature.* 381:155–158.

8. Lowe, L.A., D.M. Supp, K. Sampath, T. Yokoyama, C.V.E. Wright, S.S. Potter, P. Overbeek, and M.R. Kuehn. 1996. Conserved left-right asymmetry of nodal expression and alterations in murine *situs inversus. Nature.* 381:158–161.

9. Layton, W.M. 1976. Random determination of a developmental process. Reversal of normal visceral asymmetry in the mouse. *J. Hered.* 67:336–338.

10. Supp, D.M., D.P. Witte, S.S. Potter, and M. Brueckner. 1996. Mutation of an axonemal dynein affects left-right asymmetry in *inversus viscerum* mice. *Nature.* 389:963–966.

11. Holzbaur, E.L.F., and R. Vallee. 1994. Dyneins: molecular structure and cellular function. *Annu. Rev. Cell Biol.* 10:339–372.

12. Handel, M.A., and J.R. Kennedy. 1984. Situs inversus in homozygous mice without immotile cilia. *J. Hered.* 75:498.

13. Clark, K.L., E.D. Halay, E. Lai, and S.K. Burley. 1993. Co-crystal structure of the HNF-3/*fork head* DNA-recognition motif resembles histone H5. *Nature.* 364:412–420.

14. Weigal, D., and H. Jäckle. 1990. Fork head: a new eukaryotic DNA binding motif? *Cell.* 63:455–456.

15. Kaufmann, E., and W. Knöchel. 1996. Five years on the wings of fork head. *Mech. Dev.* 57:3–20.

16. Clevidence, D.A., D.G. Overdier, W. Tao, X. Qian, L. Pani, E. Lai, and R.H. Costa. 1993. Identification of nine tissue-specific transcription factors of the hepatocyte nuclear factor 3/forkhead DNA-binding domain family. *Proc. Natl. Acad. Sci. USA.* 90:3948–3952.

17. Hackett, B.P., S.L. Brody, M. Liang, I.D. Zeitz, L.A. Bruns, and J.D. Gitlin. 1995. Primary structure of hepatocyte nuclear factor/forkhead homologue 4 and characterization of gene expression in the developing respiratory and reproductive epithelium. *Proc. Natl. Acad. Sci. USA.* 92:4249–4253.

18. Lim, L., H. Zhou, and R.H. Costa. 1997. The winged helix transcription factor HFH-4 is expressed during choroid plexus epithelial development in the mouse embryo. *Proc. Natl. Acad. Sci. USA.* 94:3094–3099.

19. Pelletier, G.J., S.L. Brody, H. Liapis, R.A. White, and B.P. Hackett. 1998. A human forkhead/winged-helix transcription factor expressed in developing pulmonary and renal epithelium. *Am. J. Physiol.* 274:L351–L359.

20. Brody, S.L., B.P. Hackett, and R.A. White. 1997. Structural characterization of the mouse *hfh-4* gene, a developmentally regulated forkhead family member. *Genomics.* 45:509–518.

21. Nagy, A., J. Rossant, R. Nagy, W. Abramow-Newerly, and J.C. Roder. 1993. Derivation of completely cell culture-derived mice from early passage embryonic stem cells. *Proc. Natl. Acad. Sci. USA.* 90:8424–8428.

22. Hackett, B.P., and J.D. Gitlin. 1992. Cell-specific expression of a Clara cell secretory protein-human growth hormone gene in the bronchiolar epithelium of transgenic mice. *Proc. Natl. Acad. Sci. USA.* 89:9079–9083.

23. Hackett, B.P., N. Shimizu, and J.D. Gitlin. 1992. Clara cell secretory protein gene expression in bronchiolar epithelium. *Am. J. Physiol.* 262:L399–L404.

24. Carmi, R., J.A. Boughman, and K.R. Rosenbaum. 1992. Human situs determination is probably controlled by several different genes. *Am. J. Med. Genet.* 44:246–247.

25. Casey, B., M. Devoto, K.L. Jones, and A. Ballabio. 1993. Mapping a gene for familial situs abnormalities to human chromosome Xq24-q27.1. *Nat. Genet.* 5:403–407.

26. Wilson, G.N., J.P. Stout, N.R. Schneider, S.M. Zneimer, and L.C. Gilstrap. 1991. Balanced translocation 12/13 and situs abnormalities: homology of early pattern formation in man and lower organisms? *Am. J. Med. Genet.* 38:601–607.

27. Brown, N.A., and L. Wolpert. 1990. The development of handedness in left/right asymmetry. *Development.* 109:1–9.

28. Sulik, K., D.B. Dehart, T. Inagaki, J.L. Carson, T. Vrablic, K. Gesteland, and G.C. Schoenwolf. 1994. Morphogenesis of the murine node and notochordal plate. *Dev. Dyn.* 201:260–278.

29. Bellomo, D., A. Lander, I. Harragan, and N.A. Brown. 1996. Cell proliferation in mammalian gastrulation: the ventral node and notochord are relatively quiescent. *Dev. Dyn.* 205:471–485.

30. Levin, M., and N. Nascone. 1997. Two molecular models of initial left-right asymmetry generation. *Med. Hypotheses.* 49:429–435.

31. Kosaki, K., and B. Casey. 1998. Genetics of human left-right axis malformations. *Semin. Cell Dev. Biol.* 9:89–99.

32. Seo, J.-W., and N.A. Brown. 1992. Abnormal laterality and congenital cardiac anomalies. Relations of visceral and cardiac morphologies in the *iv/iv* mouse. *Circulation.* 86:642–650.

33. Icardo, J.M., and M.J. Sanchez de Vega. 1991. Spectrum of heart malformations in mice with situs solitus, situs inversus, and associated visceral heterotaxy. *Circulation.* 84:2547–2558.

34. Shimizu, A., and M. Koto. 1992. Ultrastructure and movement of the ependymal and tracheal cilia in congenitally hydrocephalic WIC-Hyd rats. *Child's Nerv. Syst.* 8:25–32.

35. Nolten, L.A., P.H. Steenbergh, and J.S. Sussenbach. 1996. The hepatocyte nuclear factor 3β stimulates the transcription of the human insulin-like growth factor I gene in a direct and indirect manner. *J. Biochem.* 271:31846–31854.

36. O'Brien, R.M., E.L. Noisin, A. Suwanichkul, T. Yamasaki, P.C. Lucas, J.-C. Wang, D.R. Powell, and D.K. Granner. 1995. Hepatic nuclear factor 3- and hormone-regulated expression of the phosphoenolpyruvate carboxykinase and insulin-like growth factor-binding protein 1 genes. *Mol. Cell. Biol.* 15:1747–1758.

37. Ogg, S., S. Paradis, S. Gottlieb, G.I. Patterson, L. Lee, H.A. Tissenbaum, and G. Ruvkun. 1997. The Fork head transcription factor DAF-16 transduces insulin-like metabolic and longevity signals in *C. elegans. Nature.* 389:994–999.

38. Unterman, T.G., A. Fareeduddin, M.A. Harris, R.G. Goswami, A. Porcella, R.H. Costa, and R.G. Lacson. 1994. Hepatocyte nuclear factor-3 (HNF-3) binds to the insulin response sequence in the IGF binding protein-1 (IGFBP-1) promoter and enhances promoter function. *Biochem. Biophys. Res. Commun.* 203:1835–1841.